A&A 489, 1329–1335 (2008)
DOI: 10.1051/0004-6361:200809758

Astronomy & Astrophysics

The instability transition for the restricted 3-body problem

I. Theoretical approach

J. Eberle[1], M. Cuntz[1,2], and Z. E. Musielak[1,3]

[1] Department of Physics, Science Hall, University of Texas at Arlington, Arlington, TX 76019-0059, USA
e-mail: [wjeberle;cuntz;zmusielak]@uta.edu
[2] Institut für Theoretische Astrophysik, Universität Heidelberg, Albert Überle Str. 2, 69120 Heidelberg, Germany
[3] Kiepenheuer-Institut für Sonnenphysik, Schöneckstr. 6, 79104 Freiburg, Germany

Received 10 March 2008 / Accepted 24 June 2008

ABSTRACT

Aims. We study the onset of orbital instability for a small object, identified as a planet, that is part of a stellar binary system with properties equivalent to the restricted three body problem.
Methods. Our study is based on both analytical and numerical means and makes use of a rotating (synodic) coordinate system keeping both binary stars at rest. This allows us to define a constant of motion (Jacobi's constant), which is used to describe the permissible region of motion for the planet. We illustrate the transition to instability by depicting sets of time-dependent simulations with star-planet systems of different mass and distance ratios.
Results. Our method utilizes the existence of an absolute stability limit. As the system parameters are varied, the permissible region of motion passes through the three collinear equilibrium points, which significantly changes the type of planetary orbit. Our simulations feature various illustrative examples of instability transitions.
Conclusions. Our study allows us to identify systems of absolute stability, where the stability limit does not depend on the specifics or duration of time-dependent simulations. We also find evidence of a quasi-stability region, superimposed on the region of instability, where the planetary orbits show quasi-periodic behavior. The analytically deduced onset of instability is found to be consistent with the behavior of the depicted time-dependent models, although the manifestation of long-term orbital stability will require more detailed studies.

Key words. stars: binaries: general – celestial mechanics – stars: planetary systems

1. Introduction

More than thirty years have passed since Heppenheimer (1974) presented a preliminary theory of planet formation in binary systems, leading to the conclusion that planet formation is virtually impossible in binary systems with separation distances of less than 30 AU. Today, observations have been reported indicating that planets occur in more than twenty binary systems, as well as in several triple star systems (Patience et al. 2002; Eggenberger et al. 2004; Eggenberger & Udry 2007). Although most planets are found in wide binaries, four cases of planets in binaries with separation distances between 20 and 25 AU have also been identified[1], which are: GJ 86 (Queloz et al. 2000; Lagrange et al. 2006), γ Cep (Hatzes et al. 2003; Neuhäuser et al. 2007), HD 41004A (Zucker et al. 2004), and HD 196885A (Correia et al. 2008). The spectral type of the main stellar component ranges between F8V and K2V. These findings are consistent with previous theoretical results showing that planets can successfully form in binary (and possibly multiple) stellar systems (e.g., Kley 2001; Quintana et al. 2002), known to occur in high frequency in the local Galactic neighborhood (Duquennoy & Mayor 1991; Lada 2006; Raghavan et al. 2006).

Bonavita & Desidera (2007) performed a statistical analysis of binaries and multiple systems concerning the frequency of hosting planets, leading to the conclusion that there is no significant statistical difference between binary systems and single stars. That planets in binary systems are now considered to be relatively common is also implied by the recent detection of debris disks in various main-sequence stellar binary systems by the *Spitzer Space Telescope* (e.g., Trilling et al. 2007, and references therein). Trilling et al. observed 69 main-sequence binary star systems and found emission in excess of predicted photospheric flux levels for approximately 9% and 40% of these systems at 24 and 70 μm, respectively, interpreted as being caused by protoplanetary dust.

In the past few decades, significant progress has been made in the study of the stability of planetary orbits in stellar binary systems. Most of these studies focused on S-type systems, where the planet is orbiting one of the stars, and the second star is considered a perturbator. Conversely, P-type orbits lie well outside the binary system, where the planet essentially orbits the center of mass of both stars. Early results were obtained by Hénon & Guyot (1970), Szebehely & McKenzie (1981), Dvorak (1984, 1986), Dvorak et al. (1989), Benest (1988, 1989, 1993, 1996), Kubala et al. (1993), and Holman & Wiegert (1999), who explored the stability of planets in binary systems with different mass ratios and eccentricities. More results have been given by David et al. (2003) and Musielak et al. (2005). More recently, Mudryk & Wu (2006) and Barnes & Greenberg (2007) focused on the role of resonances in the ejection of planets, whereas

[1] In case of HD 41004A, the planet is actually a member of a highly hierarchic quadruple system.

Fatuzzo et al. (2006) presented a detailed statistical analysis of ejection times in response to a large number of configurations, concerning both the planet and the companion star.

In previous work (Stuit 1995; Musielak et al. 2005), we studied the stability of S-type orbits in stellar binary systems, and deduced the orbital stability limits for planets. These limits were found to depend on the stellar mass ratios, a result that will be explored further in this paper. We considered initially circular planetary orbits and classified them by using the following criteria: 0% ≤ truly stable ≤5%, 5% < stable ≤ 15%, 15% < marginally stable < 35%, and unstable ≥ 35%, where the percentage refers to the orbital variability with respect to the initial distance between the primary star and the planet specified at the beginning of the calculations. The stability limit of 5% was motivated by this limit being required for Earth to remain within the conservative habitable zone around the Sun (e.g., Kasting et al. 1993; Underwood et al. 2003). The limit of 35% was based on our studies that showed that test planets outside that limit were not confined to their binary system.

Our paper is structured as follows. In Sect. 2, we present the theoretical approach adopted in our study. Case studies for planets in selected stellar binary systems are given in Sect. 3. Section 4 presents our conclusions.

2. Theoretical approach

2.1. Definition

In the following, we consider the so-called coplanar circular restricted three body problem (e.g., Szebehely 1967; Roy 2005), which is defined as follows. Two stars are in circular motion about their common center of mass and their masses are much larger than the mass of the planet. In our case, the planetary mass is assumed to be 1×10^{-6} of the mass of the star it orbits; also note that the planetary motion is constrained to the orbital plane of the two stars. Moreover, it is assumed that the initial velocity of the planet is in the same direction as the orbital velocity of its host star, which is the more massive of the two stars, and that the starting position of the planet is to the right of the primary star (3 o'clock position), along the line joining the binary components (see Fig. 1).

2.2. Basic equations

The origin of the coordinate system is chosen at the center of mass of the two binary stars. Therefore, we find

$$M_1 R_1 = M_2 R_2 \tag{1}$$

with index 1 referring to the star of greater or equal mass, placed to the right, and index 2 referring to the star placed to the left in all forthcoming figures. All quantities are assumed to have their usual meaning, except as noted otherwise. The motion of the binary stars is taken to be circular. The basic setup is depicted in Fig. 1.

Considering the law of gravity, we find

$$V_i^2 = R_i \frac{GM_j}{D^2} = R_i^2 \omega^2 \tag{2}$$

with $i = 1, 2$, $j = 3-i$, $D = R_1+R_2$, V_i as velocity of star i relative to the center of mass, and ω as the angular frequency. With $M = M_1 + M_2$ as combined mass of stars 1 and 2, Kepler's third law reads as $\omega^2 = GM/D^3$ with G as the gravitational constant. The total mass of the binaries and their separation distance affect the period of motion, with $M = 10\ M_\odot$ and $D = 10$ AU, resulting in a binary orbital period of 10 years. The stellar mass ratio is defined as the mass of the smaller star to the total mass of both stars $\mu = M_2/M$. With $\alpha = 1 - \mu$, we find $M_1 = \alpha M$, $R_1 = \mu D$, $M_2 = \mu M$ and $R_2 = \alpha D$.

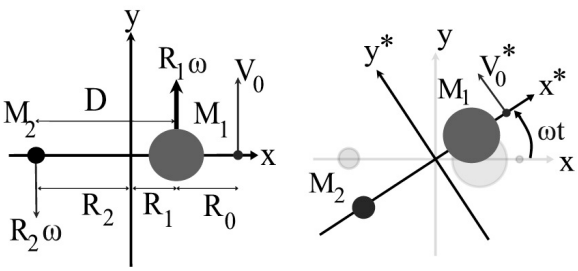

Fig. 1. Setup for the circular restricted three body problem.

Next we describe the equations of motion in fixed (sidereal) coordinates loosely following Szebehely (1967), Danby (1988), and Roy (2005). This consists in computating the orbital positions of stars 1 and 2 as a function of time t, assuming that the stars move in circular motion. These positions are denoted as $X_1(t)$, $Y_1(t)$, $X_2(t)$ and $Y_2(t)$, respectively. Furthermore, we consider a small object, a planet, with mass m_3 subjected to the gravity of both stars. The distance of the planet to star $i = 1, 2$ is given as

$$r_i(t) = \left[(X_3(t) - X_i(t))^2 + (Y_3(t) - Y_i(t))^2\right]^{\frac{1}{2}} \tag{3}$$

with X_3 and Y_3 as (sidereal) coordinates of the planet. By introducing the potential energy of the planet and applying Newton's law, we obtain

$$\begin{aligned} \ddot{X}_3 &= -\frac{GM_1}{{r_1}^3}(X_3 - X_1) - \frac{GM_2}{{r_2}^3}(X_3 - X_2) \\ \ddot{Y}_3 &= -\frac{GM_1}{{r_1}^3}(Y_3 - Y_1) - \frac{GM_2}{{r_2}^3}(Y_3 - Y_2). \end{aligned} \tag{4}$$

The distance D between the binary stars is useful as a scale factor to normalize distances using $X_3 = Dx_3$ and $Y_3 = Dy_3$. Thus, the dimensionless position vector for the small mass in the sidereal reference frame is given as (x_3, y_3). The dimensionless time τ is introduced as $\tau = \omega t$. The dimensionless representation of the velocity and acceleration for the planet is given as $\mathrm{d}X_3/\mathrm{d}t = D\omega\dot{x}_3$ and $\mathrm{d}^2X_3/\mathrm{d}t^2 = D\omega^2\ddot{x}_3$, respectively. Equivalent equations hold for the variables in the y direction. Thus we find

$$\begin{aligned} \ddot{x}_3 &= -\left(\frac{\alpha}{{r_1}^3}(x_3 - \mu\cos\tau) + \frac{\mu}{{r_2}^3}(x_3 + \alpha\cos\tau)\right) \\ \ddot{y}_3 &= -\left(\frac{\alpha}{{r_1}^3}(y_3 - \mu\sin\tau) + \frac{\mu}{{r_2}^3}(y_3 + \alpha\sin\tau)\right) \end{aligned} \tag{5}$$

with

$$\begin{aligned} r_1(t) &= [(x_3(t) - \mu\cos\tau)^2 + (y_3(t) - \mu\sin\tau)^2]^{\frac{1}{2}} \\ r_2(t) &= [(x_3(t) + \alpha\cos\tau)^2 + (y_3(t) + \alpha\cos\tau)^2]^{\frac{1}{2}}. \end{aligned} \tag{6}$$

This set of equations constitutes the dimensionless form of the equations of motion using fixed (sidereal) coordinates.

2.3. Jacobi's integral and constant

The next step consists in transforming the equations of motion into a rotating (synodic) coordinate system that rotates along

with the binary stars, which simplifies the restricted three body problem. The binary stars remain fixed in such a coordinate system. In addition, fixed equilibrium points (Lagrange points) can be found at which the small mass rotates in sync with the binary stars.

In the synodic coordinate system, with all distances labeled by an asterisk (∗), we find

$$\frac{\partial\overline{\phi}}{\partial x_3^*} = \dot{x}_3^* - 2\dot{y}_3^* = x_3^* - \frac{\alpha}{{r_1}^3}(x_3^* - \mu) - \frac{\mu}{{r_2}^3}(x_3^* + \alpha)$$

$$\frac{\partial\overline{\phi}}{\partial y_3^*} = \ddot{y}_3^* + 2\dot{x}_3^* = \left(1 - \frac{\alpha}{{r_1}^3} - \frac{\mu}{{r_2}^3}\right) y_3^* \tag{7}$$

with the dimensionless distances to each star given as

$$r_1(t) = [(x_3^*(t) - \mu)^2 + y_3^*(t)^2]^{\frac{1}{2}}$$
$$r_2(t) = [(x_3^*(t) + \alpha)^2 + y_3^*(t)^2]^{\frac{1}{2}}. \tag{8}$$

Equation (7) is written as a gradient of a scalar pseudo-potential $\overline{\phi}$, and by integration by quadrature we obtain

$$\overline{\phi} = \frac{1}{2}\left[\left(x_3^{*2} + y_3^{*2}\right) + 2\left(\frac{\alpha}{r_1} + \frac{\mu}{r_2}\right)\right], \tag{9}$$

as well as the identity

$$\frac{1}{2}\left(\dot{x}_3^{*2} + \dot{y}_3^{*2}\right) = \overline{\phi} - \frac{\overline{C}}{2} \tag{10}$$

where $\overline{C}$ constitutes a constant of integration.

For the small mass, the dimensionless distance from the center of mass and the synodic velocity are

$$r(\tau) = \left[x_3^{*2}(\tau) + y_3^{*2}(\tau)\right]^{\frac{1}{2}}$$

$$v^*(\tau) = \left[\dot{x}_3^{*2}(\tau) + \dot{y}_3^{*2}(\tau)\right]^{\frac{1}{2}}, \tag{11}$$

which allows rewriting Eq. (10) as

$$v^{*2} = 2\overline{\phi} - \overline{C} = r^2 + 2\left(\frac{\alpha}{r_1} + \frac{\mu}{r_2}\right) - \overline{C}. \tag{12}$$

This is an integral of motion in the rotating cartesian coordinate system known as Jacobi's integral.

The constant $\overline{C}$ can be set by the system parameters μ and α, noting that $\alpha = 1 - \mu$, and the initial conditions. Jacobi's integral constitutes a relationship between the velocity and position of the planet that remains unchanged during the time-dependent development of the system. It can also be shown that Jacobi's integral at the L_4 and L_5 equilibrium positions can be utilized to specify the Jacobi constant C, given as $C = \overline{C} + \mu(1 - \mu)$. This results in an absolute minimum at L_4 and L_5 for any μ, which is useful when comparing the characteristic behavior of C for various initial conditions.

The system parameters μ and α and the initial conditions, allowing v_0^* to be set, can also be used to formulate an expression for the Jacobi constant C, which is

$$C = 2\left[\alpha\left(\frac{{\rho_0}^3 + 2}{2\rho_0}\right) + \mu\left(\frac{(1+\rho_0)^3 + 2}{2(1+\rho_0)}\right)\right] - {v_0^*}^2 \tag{13}$$

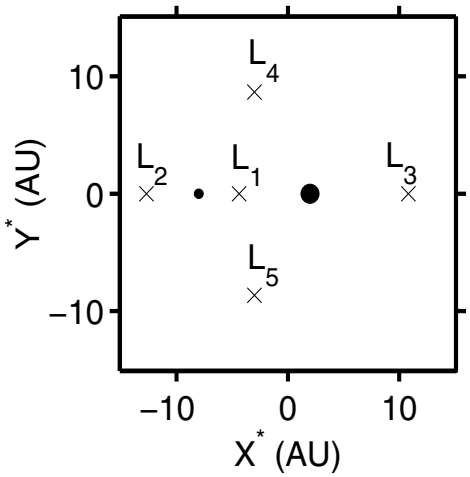

Fig. 2. Locations of the Lagrange points L_1, L_2, L_3, L_4, and L_5 in synodic coordinates X^* and Y^*.

where $\rho_0 = R_0/D$ is the planet's relative initial distance (see Fig. 1) and v_0^* is the planet's initial velocity in the rotating coordinate system.

The initial velocity is set by adding the initial velocity of the primary star $R_1\omega$ to the velocity that would result in a circular orbit about a stationary star. This allows the Jacobi constant to be expressed as

$$C = \mu + 2\mu\rho_0 + \frac{1-\mu}{\rho_0} + \frac{2\mu}{1+\rho_0} + 2\sqrt{\rho_0(1-\mu)}. \tag{14}$$

Obviously, the Jacobi constant depends solely on the parameters μ and ρ_0 of the star-planet system, and not on any orbital parameter attained during the course of the simulation. This latter property is a further confirmation that C will not change with time.

2.4. The Jacobi constants at L_1, L_2, and L_3

If we consider the situation when the net force acting on the planet is zero, including fictitious centrifugal forces due to the rotation of the non-inertial synodic reference frame, then the planet will have zero acceleration in that frame, resulting in an equilibrium position. There is a total of five solutions. The five equilibrium points are commonly known as Lagrange points L_1, L_2, L_3, L_4, and L_5 (see Fig. 2). Following Danby (1988), L_1 is located between the primary and secondary stars, and L_2 and L_3 are located to the left of the secondary star and to the right of the primary star, respectively; note that in some textbooks these three Lagrange points are defined differently (e.g., Roy 2005).

The relevance of the points L_1, L_2, and L_3 to the problem considered here is that the values of the Jacobi's constants, C_1, C_2, and C_3, corresponding to these points are useful for establishing the stability of planetary orbits in the system. According to Danby (1988) and Roy (2005), the constants obey the following relation: $C_3 < C_2 < C_1$. Specifically, if $C < C_1$, then a planet initially orbiting the primary star may be captured by the secondary star. If $C < C_2$, then the planet is free to escape from the system through point L_2. Finally, if $C < C_3$, then the planet may also escape from the system through point L_3.

In the following, we calculate C_1, C_2, and C_3, and use them to determine $\rho_0^{(1)}$, $\rho_0^{(2)}$, and $\rho_0^{(3)}$ (see Table 1), which represent critical values of the planet's relative initial distance ρ_0 in correspondence to the different types of planetary orbital stability

Table 1. Characteristic planet distances.

μ	$\rho_0^{(1)}$	$\rho_0^{(2)}$	$\rho_0^{(3)}$
0.50	0.251	0.442	0.442
0.40	0.278	0.406	0.512
0.30	0.311	0.404	0.593
0.20	0.353	0.420	0.692
0.10	0.423	0.466	0.820
0.01	0.637	0.648	0.979

Note: $\rho_0^{(i)}$ denotes the planet's initial distance ρ_0 where the Jacobi constant C is equal to C_i.

Table 2. Tests of computer code.

n	μ	τ [yr step^{-1}]	$T_{\rm sim}$ [yr]	$T_{\rm run}$ [min]	ϵ [AU]
1	1×10^{-3}	5×10^{-6}	50	10^0	10^0
2	1×10^{-3}	5×10^{-7}	50	10^1	10^{-1}
3	1×10^{-3}	5×10^{-8}	50	10^2	10^{-2}
4	1×10^{-3}	5×10^{-9}	50	10^3	10^{-3}

discussed above. These values of $\rho_0^{(i)}$ will only depend on the stellar mass ratio μ (see Table 1); i.e., the $\rho_0^{(i)}$ increase when μ decreases. The planet's absolute stability is guaranteed only if $\rho_0 < \rho_0^{(1)}$; in this case, the planet moves about the primary star in a periodic orbit. The criteria for planetary orbits to be unstable are either $\rho_0 > \rho_0^{(2)}$ or $\rho_0 > \rho_0^{(3)}$, or both. An interesting case occurs if $\rho_0 > \rho_0^{(1)}$ and $\rho_0 < \rho_0^{(2)}$. The existence of periodic orbits in this case depends on the value of C (e.g., Szebehely 1967; Danby 1988; Roy 2005, and references therein).

In this paper, we describe case studies for binary systems of different mass ratios μ. Our focus is to obtain insight into planetary orbital stability, especially the transition to unstable orbits.

2.5. Tests of computer code

The accuracy of the computer code utilized for pursuing our simulations is checked by integrating the equations of motion for a small body placed near the triangular L_4 point. A mass ratio of $\mu = 0.001$ is assumed considering that the triangular Lagrange points are only stable for $\mu \le \mu_0 = 0.0385 = (1 - \sqrt{69}/9)/2$ (Szebehely 1967). If the small mass is placed near the stable point, it will oscillate about that point. Even if in the simulation it could be placed exactly at the stable point, an impossible task owing to the truncation errors inherit in any digital variable, the Runge-Kutta integrator would still introduce an error proportional to the size of the time step τ of $O(\tau^5)$ for each step, but $O(\tau^4)$ over multiple steps. This means that shorter time steps will keep the body more closely near the stable point, but will extend the running time of the simulation.

In Table 2, it is shown how different values of τ affect the precision and running time of the simulation. The approximate scale of the motion about the stable point is given by the quantity ϵ. Here $T_{\rm sim}$ is the physical time of the simulation, and $T_{\rm run}$ the computational time of the simulation to run on a Pentium 4 CPU Dual 3 GHz with 1 GB RAM. For shorter time steps, the deviation from the equilibrium is less; however, the time it takes to run the simulation increases by the same magnitude.

As depicted in Table 2, $T_{\rm sim}$ is 50 yr corresponding to five orbits of the binary system. This is the same simulation time as used for the bulk of simulations undertaken as part of a broad qualitative scan of the system for different mass ratios and initial conditions. We used a time step of 5×10^{-7} yr step^{-1} because it allowed a quick survey of the parameter space with an error accumulation of the motion of the small planet given as $\epsilon/D \simeq 1\%$. However, this may be slightly misleading because the amount of error accumulation is highly dependent on the stability of the respective point. The error accumulation in the simulations will most likely be greater for cases in which instability occurs.

Since this test of accuracy was done only for a known stable point, we also investigated a few simulations on quasi-stable orbits with the same time steps as used in the 50 year simulations, as well as with time steps an order of magnitude smaller for simulation times of up to 1000 years corresponding to 100 binary orbits with no discernable difference. Moreover, the validity of our method is also confirmed by the fact that one of the case studies (i.e., $\mu = 0.1$, $\rho_0 = 0.461$) has previously been discussed by Szebehely (1967) who found very similar results to those given in this paper.

3. Case studies of planetary motion

In Figs. 3, 4, and 5, we illustrate the transition from stability to instability by progressively increasing the value of ρ_0, i.e., the relative distance of the planet from the primary star, for binary systems with a fixed mass ratio μ, given as $\mu = 0.5$, 0.3, and 0.1, respectively; see Cuntz et al. (2007) and Eberle et al. (2008) for results concerning $\mu = 0.2$. While the initial distance of the planet from its host star is increased, the initial velocity of the planet is set assuming initially circular orbits. Moreover, the changes in the potential and kinetic energies of the planet due to increased values of ρ_0 widen the domain for the possible planetary motion, as reflected by the increase in space between the zero velocity curves. If ρ_0 is increased beyond $\rho_0^{(1)}$, $\rho_0^{(2)}$, and $\rho_0^{(3)}$, the zero velocity contour opens at L_1, L_2, and L_3, respectively, which dramatically affects the orbital stability of the planet.

Figure 3 focuses on models with $\mu = 0.5$, where both stars have equal mass. Here we study the cases of $\rho_0 = 0.200$, 0.300, 0.425, and 0.450. For $\rho_0 = 0.200$, the planet's absolute stability is guaranteed since $\rho_0 < \rho_0^{(1)}$ with $\rho_0^{(1)}$ given as 0.251 (see Table 1). For the case of $\rho_0 = 0.300$, an extreme case of orbital instability is encountered, as the planet follows a highly intricate quasi-chaotic orbit; obviously, the planet is orbiting each star in a highly unpredictable manner. A very interesting case occurs for $\rho_0 = 0.425$. Even though planetary orbital stability is not guaranteed, the planet nevertheless follows a quasi-periodic orbit, at least for the very short time of our orbital simulations (50 yr). For that particular value of ρ_0, the zero velocity contour is close to opening at both L_2 and L_3, and the planet is now on the brink of being able to escape from the system entirely. For $\rho_0 = 0.450$, instability is observed again. However, even though it would be possible for the planet to leave the system due to its energetics, it happens that the planet is captured by the secondary star after 45.9 yr. We also did simulations for $\mu = 0.4$ (not shown here), and found a behavior due to changes in ρ_0 that is very similar to $\mu = 0.5$.

Model simulations for $\mu = 0.3$ are depicted in Fig. 4. Here we study the cases of $\rho_0 = 0.277$, 0.400, 0.474, and 0.610. In accord to our previous discussion, orbital stability is found for $\rho_0 = 0.277$ (see Table 1). For the other three cases, orbital stability is no longer secured, which means that unstable orbits are expected. However, for $\rho_0 = 0.400$ and 0.474, the planetary orbit follows quasi-periodic behavior, as also found for $\mu = 0.5$ and

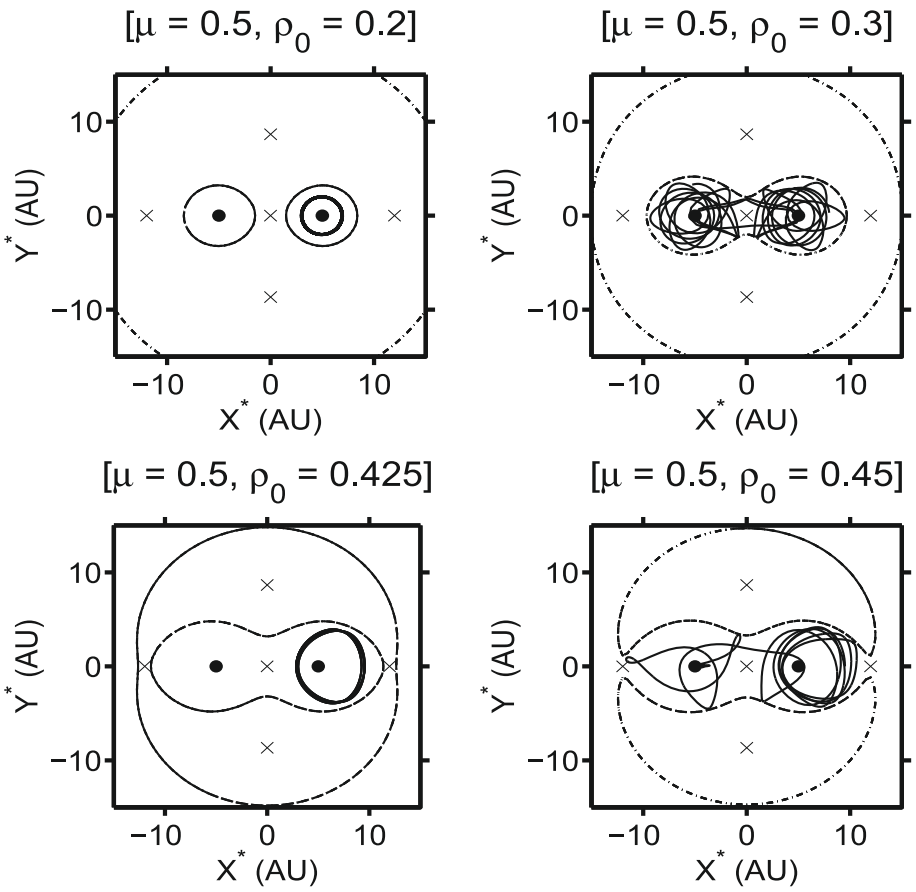

Fig. 3. For a mass ratio of $\mu = 0.5$, runs for four different distance ratios are shown, which are $\rho_0 = 0.200$, 0.300, 0.425, and 0.450 (solid lines). We also show the zero velocity contours (dash-dotted lines) indicating the permitted regions of motion and the Lagrange points (crosses).

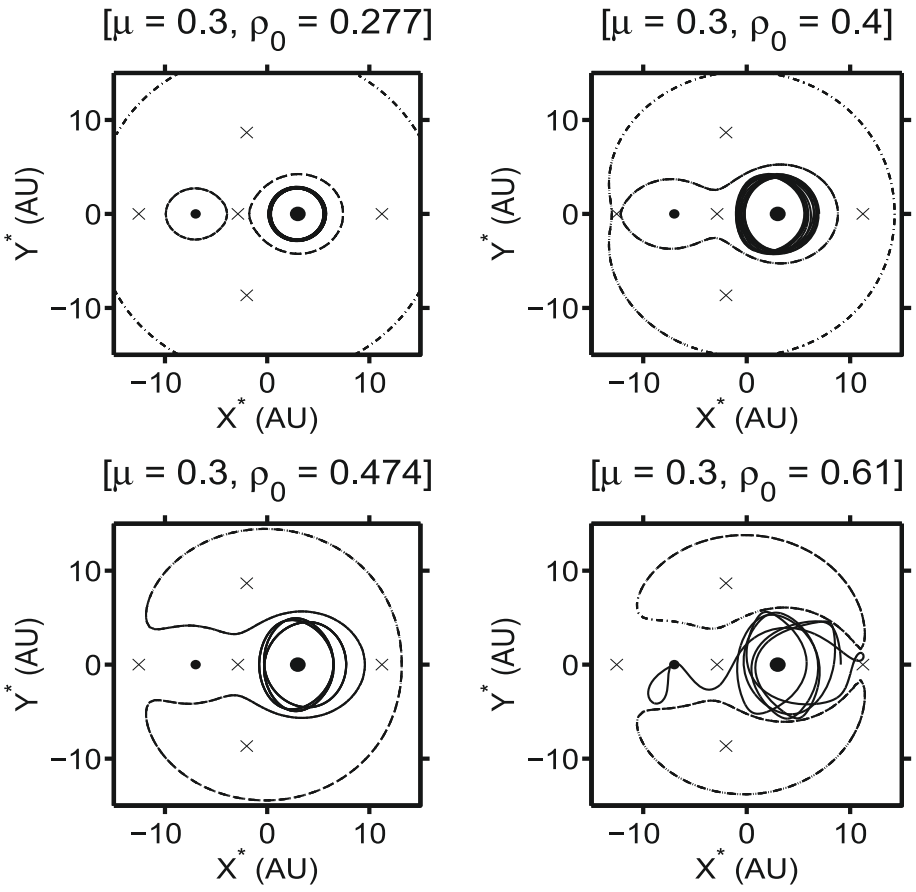

Fig. 4. Same as Fig. 3, but now for a mass ratio of $\mu = 0.3$ and distance ratios of $\rho_0 = 0.277$, 0.400, 0.474, and 0.610.

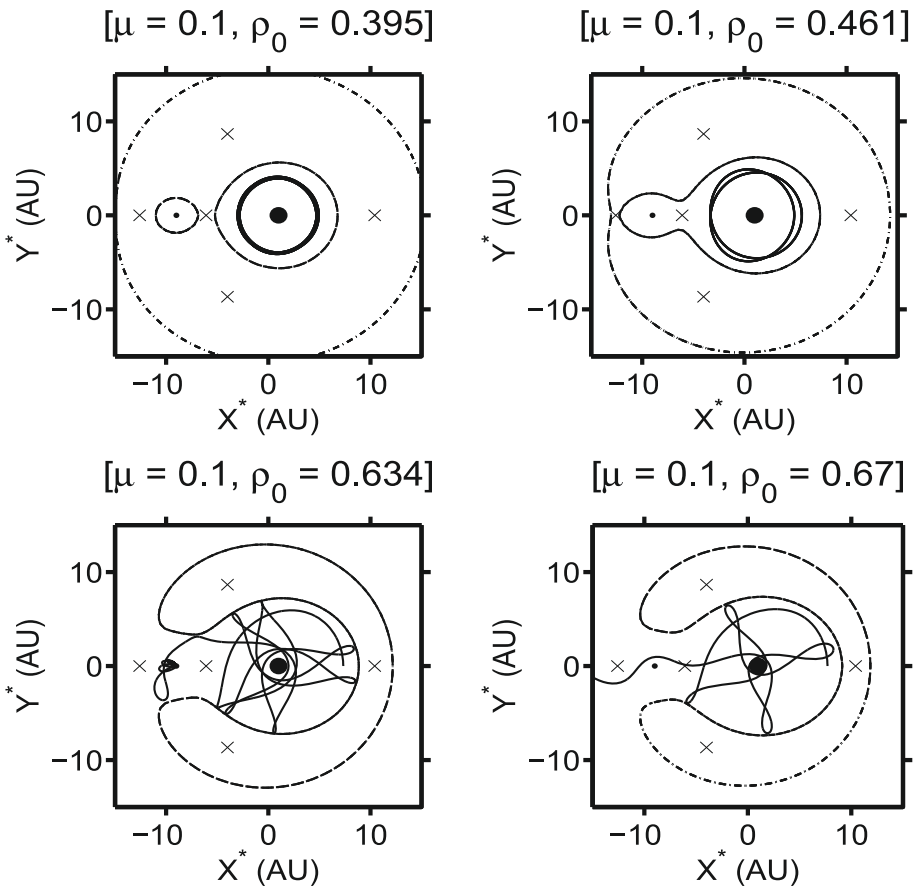

Fig. 5. Same as Fig. 3, but now for a mass ratio of $\mu = 0.1$ and distance ratios of $\rho_0 = 0.395$, 0.461, 0.634, and 0.670.

$\rho_0 = 0.425$ (see Fig. 6). For $\rho_0 = 0.610$, a complicated planetary orbit emerges. Although the planet is in principle able to leave the binary system entirely, as implied by the topology of the zero velocity contour, it is found that it loops around L_3 between an elapsed time of 35 and 39 yr, and that it is captured by the secondary star after 45.8 yr.

As examples for low mass ratios, we study $\mu = 0.1$ (see Fig. 5) for the cases of $\rho_0 = 0.395$, 0.461, 0.634, and 0.670. Note that the difference between $\rho_0^{(1)}$ and $\rho_0^{(2)}$ is very small and, consequently, the initial conditions that result in zero velocity curves passing through L_1 and L_2 are close to each other. As the mass ratio approaches zero, the values of C_1 and C_2 approach each other much more quickly than C_3. This implies that even though the range of initial conditions for which $\rho_0 < \rho_0^{(1)}$ is wide, once $\rho_0^{(1)}$ is passed, the transition to significant instability occurs well prior to ρ_0 approaching $\rho_0^{(3)}$. Our studies find orbital stability for $\rho_0 = 0.395$ and quasi-periodicity for $\rho_0 = 0.461$. For $\rho_0 = 0.461$, this result is consistent with previous analytical work by Szebehely (1967), which constitutes an indirect validation of our adopted numerical and analytical methods. For $\rho_0 = 0.634$, the planet approaches the zero velocity contour after about 28 yr, and is caputured by the secondary star after 35.1 yr. For $\rho_0 = 0.670$, it is found that the planet passes by the secondary star after about 18 yr, and thereafter continues to escape from the system.

Our simulations indicate that, when the mass ratio is small, i.e., $\mu < 0.4$, the planet appears to remain in a stable, yet peculiar, orbit about the more massive star, well beyond the point at which the zero velocity curve has first opened up. Instability seems to occur when the orbit of the planet comes very close to the zero velocity curve. In this case, it abruptly changes direction and falls toward the more massive star, whereupon it is catapulted in a new direction and the probability of capture

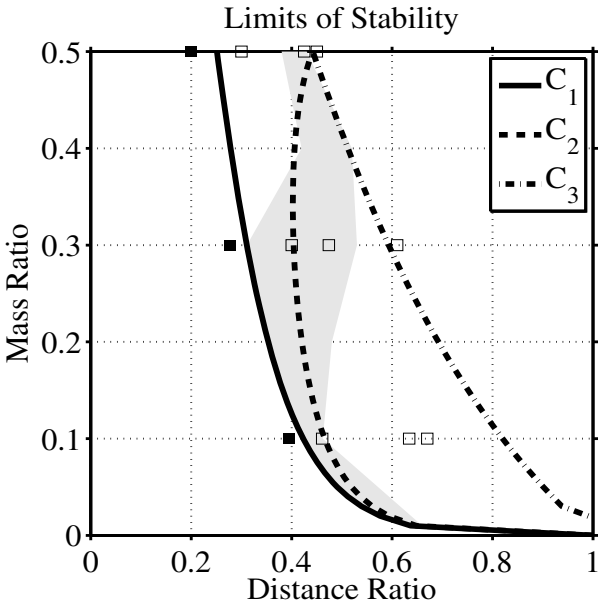

Fig. 6. Limits of stability for planetary orbits for different mass ratios μ. We show the results based on Jacobi's constant C_1 (solid line) (criterion of stability) and based on Jacobi's constant C_2 (dashed line) and C_3 (dash-dotted line). In addition, we indicate the model parameters μ and ρ_0 of the simulations depicted in Figs. 3 to 5. Here the filled and open boxes refer to case studies of orbital stability and instability, respectively. The gray area indicates the domain of quasi-stability, tentatively determined by our model simulations.

increases. However, for a given parameter combination of (μ, ρ_0), it is nonetheless difficult to gauge when this is going to occur because there is no obvious way of determining how close the planet has to come to the zero velocity curve for its trajectory to be deflected.

Based on our studies, highly intricate orbits are encountered for $\rho_0 = 0.300$ and 0.450 in the case of $\mu = 0.5$, for $\rho_0 = 0.610$ in case of $\mu = 0.3$ and, furthermore, for $\rho_0 = 0.634$ and 0.670 in the case of $\mu = 0.1$. In these model simulations, the initial distance of the planet from its host star (i.e., the primary star of the binary system) is sufficiently large to be able to initiate orbital instability. This is indicated by the fact that the respective ρ_0 value of the model is above the ρ_0 value associated with the C_1, C_2, or C_3 limit, or two or more of these limits (see Fig. 6). In some other cases, quasi-periodic orbits are found, even though the planet is expected to follow an unstable orbit, based on the condition previously discussed. This phenomenon will be studied in more detail in Paper II of this series.

4. Conclusion

For the coplanar circular restricted three body problem, we developed stringent mathematical criteria that permit insight into the orbital stability of planets in a stellar binary system. This is accomplished by comparing the planet's relative initial distance ρ_0 to the critical values $\rho_0^{(1)}$, $\rho_0^{(2)}$, and $\rho_0^{(3)}$, defined for a fixed stellar mass ratio μ. An adequate way of demonstrating the different types of behavior is to assess the topology of the zero velocity contour, defined by the μ and ρ_0 values of the system.

The orbital stability of a planet is ensured if its orbit is entirely encapsulated by the zero velocity contour, a result previous pointed out by Roy (2005) and others. The rationale of the zero velocity contour is that it limits the allowable region of the planet as dictated by its limited available kinetic energy. As part of this study, we illustrate the onset of planetary instability by sets of model simulations with different initial planetary starting positions for systems with a given mass ratio. The property of the planet to remain within the zero velocity contour is tantamount to orbital stability, although it does not necessarily imply stability in the sense of quasi-periodicity. Based on the very short timespan of our simulations, we encountered evidence that quasi-periodic orbits may even occur for planets outside the previously established stability region. The relationship between these two stability assessments will be investigated in more detail in Paper II.

Previous numerical case studies (e.g., Holman & Wiegert 1999; Musielak et al. 2005; David et al. 2003) show a behavior consistent with the theoretical prediction of a stringent stability limit, although some minor, but noticeable, differences exist (see discussion by Cuntz et al. 2007), which are typically attributable to minor shortcomings in the analytical fitting procedure owing to the time limitation of the numerical simulations. Note however that for generalized binary systems, other methods are required to establish long-term stability of planetary orbits. Important applications of our work include evaluating numerically deduced stability limits for cases where analytical results exist and obtaining insight into the onset of orbital instability, including routes to chaos.

Acknowledgements. This work has been supported by the Department of Physics, University of Texas at Arlington (J. E., M. C.), and by the Alexander von Humboldt Foundation (Z. E. M.).

References

Barnes, R., & Greenberg, R. 2007, ApJ, 665, L67
Benest, D. 1988, Celest. Mech. Dyn. Astron., 43, 47
Benest, D. 1989, A&A, 223, 361
Benest, D. 1993, Celest. Mech. Dyn. Astron., 56, 45
Benest, D. 1996, A&A, 314, 983
Bonavita, M., & Desidera, S. 2007, A&A, 468, 721
Correia, A. C. M., Udry, S., Mayor, M., et al. 2008, A&A, 479, 271
Cuntz, M., Eberle, J., & Musielak, Z. E. 2007, ApJ, 669, L105
Danby, J. M. A. 1988, Fundamentals of Celestial Mechanics (Richmond: Willmann-Bell, Inc.)
David, E.-M., Quintana, E. V., Fatuzzo, M., & Adams, F. C. 2003, PASP, 115, 825
Duquennoy, A., & Mayor, M. 1991, A&A, 248, 485
Dvorak, R. 1984, Celest. Mech. Dyn. Astron., 34, 369
Dvorak, R. 1986, A&A, 167, 379
Dvorak, R., Froeschlé, Ch., & Froeschlé, Cl. 1989, A&A, 226, 335
Eberle, J., Cuntz, M., & Musielak, Z. E. 2008, in Bioastronomy 2007: Molecules, Microbes and Extraterrestrial Life, ed. K. Meech, M. Mumma, J. Siefert, & D. Werthimer (San Francisco: ASP), ASP Conf. Proc., in press [arXiv:0712.3266]
Eggenberger, A., & Udry, S. 2007, in Planets in Binary Star Systems, ed. Haghighipour (New York: Springer), in press [arXiv:0705.3173]
Eggenberger, A., Udry, S., & Mayor, M. 2004, A&A, 417, 353
Fatuzzo, M., Adams, F. C., Gauvin, R., & Proszkow, E. M. 2006, PASP, 118, 1510
Hatzes, A. P., Cochran, W. D., Endl, M., et al. 2003, ApJ, 599, 1383
Hénon, M., & Guyot, M. 1970, Periodic Orbits, Stability and Resonances, ed. G. E. O. Giacaglia (Dordrecht: Reidel), 349
Heppenheimer, T. A. 1974, Icarus, 22, 436
Holman, M. J., & Wiegert, P. A. 1999, AJ, 117, 621
Kasting, J. F., Whitmire, D. P., & Reynolds, R. T. 1993, Icarus, 101, 108
Kley, W. 2001, in The Formation of Binary Stars, ed. H. Zinnecker, & R. D. Mathieu (San Francisco: ASP), IAU Symp., 200, 511
Kubala, A., Black, D., & Szebehely, V. G. 1993, Celest. Mech. Dyn. Astron., 56, 51
Lada, C. J. 2006, ApJ, 640, L63
Lagrange, A.-M., Beust, H., Udry, S., Chauvin, G., & Mayor, M. 2006, A&A, 459, 955
Mudryk, L. R., & Wu, Y. 2006, ApJ, 639, 423
Musielak, Z. E., Cuntz, M., Marshall, E. A., & Stuit, T. D. 2005, A&A, 434, 355
Neuhäuser, R., Mugrauer, M., Fukagawa, M., Torres, G., & Schmidt, T. 2007, A&A, 462, 777
Patience, J., White, R. J., Ghez, A. M., et al. 2002, ApJ, 581, 654
Queloz, D., Mayor, M., Weber, L., et al. 2000, A&A, 354, 99
Quintana, E. V., Lissauer, J. J., Chambers, J. E., & Duncan, M. J. 2002, ApJ, 576, 982
Raghavan, D., Henry, T. J., Mason, B. D., et al. 2006, ApJ, 646, 523
Roy, A. E. 2005, Orbital Motion (Bristol and Philadelphia: Institute of Physics Publ.)
Stuit, T. D. 1995, M.S. Thesis, University of Alabama in Huntsville
Szebehely, V. 1967, Theory of Orbits (New York and London: Academic Press)
Szebehely, V. G., & McKenzie, R. 1981, Celest. Mech. Dyn. Astron., 23, 3
Trilling, D. E., Stansberry, J. A., Stapelfeldt, K. R., et al. 2007, ApJ, 658, 1289
Underwood, D. R., Jones, B. W., & Sleep, P. N. 2003, Int. J. Astrobiol., 2, 289
Zucker, S., Mazeh, T., Santos, N. C., Udry, S., & Mayor, M. 2004, A&A, 426, 695